Discrete model predictive frequency and voltage control of isolated micro-grid in smart grid scenario

Puvvula S R V R S S Vidyasagar
Electrical engineering department
Indian Institute of Technology
Chennai, India
ee14d030@ee.iitm.ac.in

K Shanti Swarup
Electrical engineering department
Indian Institute of Technology
Chennai, India
swarup@ee.iitm.ac.in

***Abstract*—In an isolated micro-grid electronically interfaced DG (EI-DG) units should also participate in frequency and voltage control along with synchronous generator based DG (SG-DG) units to ensure power quality and stability of the micro-grid. The conventional way of controlling frequency and voltage is to balance active power and reactive power of the system by implementing droop characteristics (P-f, Q-V) for EI-DG units with PI controllers and automatic generation control (AGC) and automatic voltage regulator (AVR) for SG-DG units. With the advent of smart micro-grids, a centralized control for both frequency and voltage using model predictive controller (MPC) is an alternative to the conventional controllers. The optimization capabilities of MPC make it suitable for frequency and voltage control of micro-grids equipped with fast and reliable communication. This paper investigates the performance of a centralized discrete model predictive controller (DMPC) in an isolated micro-grid with photovoltaic (PV) and diesel generators. The small signal dynamic models of the PV converter and SG-DG are considered in the design of the DMPC. The micro-grid network and loads are represented using steady state power balance equations. The performance of the DMPC is tested using MATLAB software package.**

Keywords—isolated micro-grid;model predictive controller; small signal model; frequency control; voltage control; droop characteristics;

I. INTRODUCTION

Conventional power systems with large synchronous generator based power plants maintains frequency and voltage stability with the help of automatic generation control (AGC) and automatic voltage regulator (AVR). AGC controls the injected active power and AVR controls the excitation and there by controls the injected reactive power [1]. With the advent of micro-grids the aspects of frequency and voltage control are rapidly changing. A micro-grid generally consists of two or more distributed generators. The generators may be of conventional diesel or steam type or electronically interfaced renewable sources. Voltage of the micro-grid is locally controlled by generating sufficient reactive power where as frequency control is taken care by main grid in grid connected mode [2][3]. All the generators in micro-grid operate as PQ sources generating pre defined active and reactive power set-points [2-4]. In isolated micro grid environment both synchronous generator based (SG-DG) and electronically interfaced distributed generators (EI-DG) are forced to participate in frequency regulation and voltage control [4][5]. The conventional way of controlling voltage and frequency in isolated micro-grid is to force the EI-DG to follow droop characteristics (P-f, Q-V) through independent d-q current control using PI controllers [2-6]. In smart grid scenario, in the presence of fast communication devices model predictive controller (MPC) is an alternative to the conventional PI controllers for controlling voltage and frequency of isolated micro-grids. Using present state information of a system, MPC predicts the future response of the system with the help of a mathematical model of the system [7-9]. While controlling frequency and voltage many constraints are imposed on the operation of the controller especially in isolated micro-grids which can be handled by the MPC very well when compared to the other controllers [8][9]. It can exploit our knowledge about the disturbances that are affecting the frequency and voltage. This is not the case with presently used PI control methods. This paper presents a detailed approach of centralized frequency and voltage control of a photovoltaic (PV) and diesel generator based micro-grid in isolated environment using discrete model predictive controller (DMPC). The superiority of DMPC over conventional PI controller is explained using simulation results.

II. MATHEMATICAL MODEL OF MICRO-GRID

A. Micro-grid description

Micro-grid used in the present study is composed of two generators, an EI-DG unit of 2.5-MVA and a SG-DG unit of 5-MVA capacity. The EI-DG unit represents PV source interfaced with the micro-grid using voltage source converter (VSC). SG-DG represents synchronous generator coupled to turbine with diesel as input fuel. The parameters of the two DG units are given in [3]. The information about each of the component is shown in Fig. 1.

For the ease of analysis the entire micro-grid with 13 buses is represented by a three bus system shown in Fig. 2. For designing the DMPC, micro-grid linearized model is expressed in state space representation as

$$\frac{d\,\Delta x}{dt} = A\,\Delta x + B\,\Delta u \tag{1}$$

978-1-4799-5141-3/14/$31.00 ©2016 IEEE

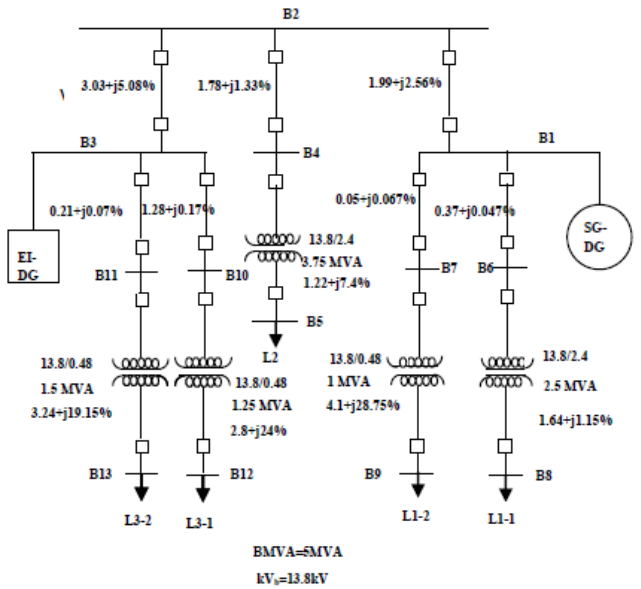

Fig.1 Micro-grid one line diagram

To construct (1), the dynamic models of the EI-DG, SG-DG, micro-grid network and loads are required. In Fig. 3, d-q is the global reference frame which is an imaginary synchronous frame rotating at the angular speed of ω_b. Initially d-axis is oriented along voltage space vector V^{G1} of bus B1. d1-q1 is the reference frame of SG-DG. It is locked to SG-DG rotor and rotates with angular speed of ω_r. q1 axis is aligned along machine internal voltage E_g. δ_0 is the power angle of SG-DG and is related to instantaneous rotor angle δ_1 of SG-DG by the equation

$$\delta_0 = \frac{\pi}{2} + \delta_1 \tag{2}$$

d3-q3 is the reference frame of EI-DG rotating at the angular speed of ω_3. d3 is always aligned along the voltage space vector v^{G3} of B3 as shown in Fig. 3. δ_3 is the instantaneous phase angle of v^{G3}.

B. SG-DG model

The SG-DG model in d1-q1 frame of reference is represented by sub transient model of the synchronous generator with stator transients neglected. The turbine model with reheater and inherent speed droop governor is considered in this study. The excitation system is a generic IEEE DC1A system. The complete model of the SG-DG in per unit (p.u.) is given by (3)-(19)

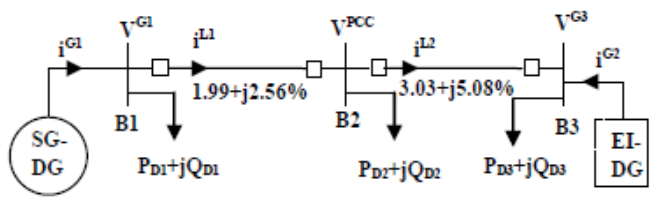

Fig. 2 Reduced micro-grid network

$$T'_{do}\frac{dE'_q}{dt} = -E'_q - (x_d - x'_d)\left[i_{d1} - \frac{(x'_d - x''_d)}{(x'_d - x_{ls})^2}\left(-E'_q + (x'_d - x_{ls})i_{d1} + \psi_{1d}\right)\right] + E_{fd} \tag{3}$$

$$T'_{qo}\frac{dE'_d}{dt} = -E'_d + (x_q - x'_q)\left[i_{q1} - \frac{(x'_q - x''_q)}{(x'_q - x_{ls})^2}\left(E'_d + (x'_q - x_{ls})i_{q1} + \psi_{2q}\right)\right] \tag{4}$$

$$T''_{qo}\frac{d\psi_{2q}}{dt} = -E'_d - (x'_q - x_{ls})i_{q1} - \psi_{2q} \tag{5}$$

$$T''_{do}\frac{d\psi_{1d}}{dt} = E'_q - (x'_d - x_{ls})i_{d1} - \psi_{1d} \tag{6}$$

$$v_{q1} + r_s i_{q1} = -x''_d i_{d1} + \frac{(x''_d - x_{ls})}{(x'_d - x_{ls})}E'_q + \frac{(x'_d - x''_d)}{(x'_d - x_{ls})}\psi_{1d} \tag{7}$$

$$-v_{d1} - r_s i_{d1} = -x''_q i_{q1} - \frac{(x''_q - x_{ls})}{(x'_q - x_{ls})}E'_d + \frac{(x'_q - x''_q)}{(x'_q - x_{ls})}\psi_{2q} \tag{8}$$

$$\frac{d\delta_1}{dt} = \omega_r - \omega_b \tag{9}$$

$$\frac{2H}{\omega_b}\frac{d\omega_r}{dt} = T_m - T_e - D(\omega_r - \omega_b) \tag{10}$$

$$T_E\frac{dE_{fd}}{dt} = V_R - (K_E + S_E(E_{fd}))E_{fd} \tag{11}$$

$$T_A\frac{dV_R}{dt} = -V_R + K_A R_F - \frac{K_A K_F}{T_F}E_{fd} + K_A(V_{ref} - V_1) \tag{12}$$

$$\frac{dR_F}{dt} = -R_F + \frac{K_F}{T_F}E_{fd} \tag{13}$$

$$T_{RH}\frac{dT_m}{dt} = -T_m + (1 - \frac{K_{HP}T_{RH}}{T_{CH}})P_{CH} + \frac{K_{HP}T_{RH}}{T_{CH}}P_{SV} \tag{14}$$

$$T_{CH}\frac{dP_{CH}}{dt} = -P_{CH} + P_{SV} \tag{15}$$

$$T_{SV}\frac{dP_{SV}}{dt} = -P_{SV} + P_{ref} - \frac{1}{R_D}(\frac{\omega_r}{\omega_b} - 1) \tag{16}$$

$$v_{d1} = V_1 \sin(\delta_0 - \theta_1) \tag{17}$$

$$v_{q1} = V_1 \cos(\delta_0 - \theta_1) \tag{18}$$

$$T_e = v_{d1}i_{d1} + v_{q1}i_{q1} \tag{19}$$

Where x_d, x_q represents d-q axis synchronous reactance. x_d', x_q' represents d-q axis transient reactance and x_d'', x_q'' represents d-q axis sub-transient reactance. x_{ls} is the stator leakage reactance. E_d', E_q' are d-q axis induced voltages. Ψ_{1d}, Ψ_{2q} are the flux linkages of damper windings of d and q axis. T_{do}', T_{qo}' are transient open circuit time constants of d-q axis. T_{do}'', T_{qo}'' are sub transient open circuit time constants. v_{d1}, v_{q1} are the terminal voltage d-q components. i_{d1}, i_{q1} are the d-q currents. H represents equivalent inertia of turbine and synchronous generator rotors. D is the frequency dependent loads damping constant. E_{fd} is the field excitation. T_{RH}, T_{CH} and T_{SV} are the reheater, steam chest and steam valve time constants respectively. K_{RH} is gain of reheater. P_{CH} and P_{SV} are the power outputs from steam chest and steam valve respectively. R_D is the droop constant of the speed governor. P_{ref} is the reference set point of the turbine model. T_m and T_e are the mechanical and electromagnetic torques. K_E and T_E are exciter gain and time constant respectively. R_F is the rate

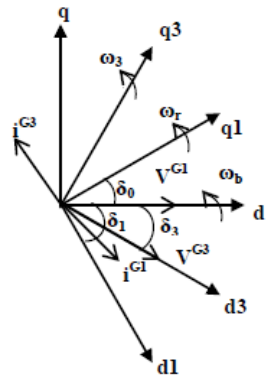

Fig. 3 Reference frames of micro-grid

feedback. K_A, T_A and V_R are voltage regulator gain, time constant and output voltage respectively. K_F and T_F are feedback transformer gain and time constant respectively. V_{ref} is the reference voltage of the regulator and V_1 is the generator terminal voltage.

C. Electronically interfaced distributed generator model

EI-DG of Fig. 2 is a PV source connected to B3 through a 3-Φ VSC. On AC side of the inverter, R_f is the p.u. value of on state switching losses, resistance of the interface transformer and filter per phase. X_f represents p.u. value of filter inductance and leakage inductance of the interface transformer per phase. The EI-DG model in its reference frame is given by

$$\frac{1}{\omega_b}\frac{di_{q3}}{dt} = \frac{-R_f}{X_f} i_{q3} - \frac{\omega_3}{\omega_b} i_{d3} + \frac{1}{X_f}(e_{q3} - v_{q3}) \tag{20}$$

$$\frac{1}{\omega_b}\frac{di_{d3}}{dt} = \frac{-R_f}{X_f} i_{d3} + \frac{\omega_3}{\omega_b} i_{q3} + \frac{1}{X_f}(e_{d3} - v_{d3}) \tag{21}$$

Where v_{d3} and v_{q3} are d3-q3 components of bus 3 voltage. i_{d3} and i_{q3} are d3-q3 components of inverter current output. e_{d3} and e_{q3} are d3-q3 components of the inverter output voltage. When d3 axis is taken in such a way that if it is oriented along the voltage space vector of bus 3, then v_{d3} and v_{q3} can be written as

$$v_{d3} = V_3 \tag{22}$$

$$v_{q3} = 0 \tag{23}$$

D. Micro-grid network model

Since the network dynamics are fast when compared to the controller and generator dynamics, network and loads in this study are represented by

$$P_{Gi} - P_{Di} = \sum_{j=1}^{3} V_i V_j Y_{ij} \cos(\theta_i - \theta_j - \alpha_{ij}) \tag{24}$$

$$Q_{Gi} - Q_{Di} = \sum_{j=1}^{3} V_i V_j Y_{ij} \sin(\theta_i - \theta_j - \alpha_{ij}) \tag{25}$$

$$P_{Gi} = v_{di} i_{di} + v_{qi} i_{qi} \quad \text{For i} = 1,3 \tag{26}$$

$$Q_{Gi} = v_{qi} i_{di} - v_{di} i_{qi} \quad \text{For i} = 1,3 \tag{27}$$

$$P_{Gi} = Q_{Gi} = 0 \quad \text{For i} = 2 \tag{28}$$

Where P_{Gi} and Q_{Gi} are generator active and reactive power output at i^{th} bus. P_{Di} and Q_{Di} are load active and reactive power demand at the ith bus. V_j and V_j are the voltages at i^{th} and j^{th} bus. θ_i and θ_j are the phase angles of ith and j^{th} bus voltage with respect to d-axis. y_{ij} is the (i,j) element of the admittance matrix with magnitude Y_{ij} and angle α_{ij}.

III. MODEL PREDICTIVE CONTROLLER FORMULATION

A. MPC description

The main function of the MPC controller is to maintain frequency and voltage stability of micro-grid by maintaining frequency and voltage within limits for the input disturbances. In the present study the disturbances are small signal load changes. While formulating the mathematical model of the MPC, number of inputs and outputs of the micro-grid are to be chosen as per the objective of the study. In the present study it is the frequency and voltage control that is to be achieved with MPC. The controller is a centralized controller and it requires the micro-grid to be smart in nature with fast data communication provided.

MPC computes trajectory of controlled future inputs of a plant to optimize the future outputs using the mathematical model of the plant. Prediction horizon is the time period or number of samples up to which outputs are to be estimated by giving plant state information at the starting time of prediction. The time up to which the future trajectories of the inputs are computed is called control horizon. It follows the receding horizon principle so that only first sample of the input is given as input to the system and for the next sampling instant the prediction and receding horizon control repeats. The entire optimization is done with regards to an objective function.

In Fig. 4 plant represents the micro-grid. MPC block contains information about the mathematical model of the micro-grid, objective function 'J', prediction horizon and control horizon. It computes the optimal system input 'u' over a fixed control horizon. The first sample of the input 'u' is given as the input to the plant and the process is continued for other samples. y_{ref} contains set-points of the outputs. The loop is closed by the measurements that include plant outputs 'y' and measurable states. State estimation block is used to calculate the states which are not measurable at each sample as the MPC needs complete state information 'x' at the starting time of prediction horizon.

B. Mathematical formulation of the MPC

The micro-grid equations from (3)-(28) are of continuous time equations. They are to be converted into discrete time and written in the form of

$$x_{disc}(k+1) = A_{disc} x_{disc}(k) + B_{disc} u(k) + B_w w(k) \tag{29}$$
$$y_{disc}(k) = C_{disc} x_{disc}(k)$$

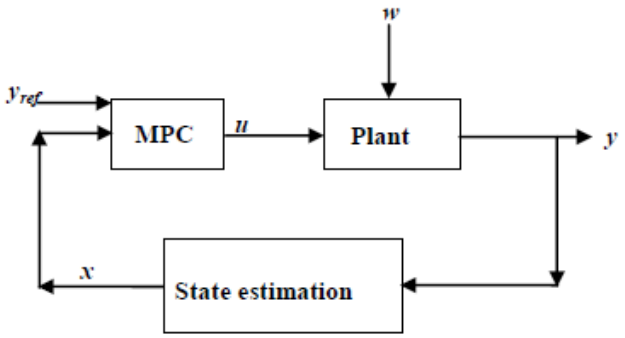

Fig. 4 MPC overview

Where x_{disc} represents a vector containing discrete states of the micro-grid, u is the control input, y_{disc} is the output vector of the plant. w is the input load disturbance vector of the plant. (A_{disc}, B_{disc}, C_{disc}) is the state space triplet in discrete form. k is the sampling instant. The discrete model is then converted into augmented state space model of the form

$$x_{aug}(k+1) = A_{aug} x_{aug}(k) + B_{aug}\,\Delta u(k) \qquad (30)$$
$$y_{disc}(k) = C_{aug}\, x_{aug}(k)$$

Where

$$x_{aug}(k) = [\Delta x_{disc}(k)^{T} \quad y_{disc}(k)^{T}]^{T}$$
$$\Delta x_{disc}(k) = x_{disc}(k) - x_{disc}(k-1)$$
$$\Delta u(k) = u(k) - u(k-1)$$

Triplet (A_{aug},B_{aug},C_{aug}) is called augmented model of the plant. Now define two vectors of the form

$$Y_{est} = \left[y_{disc}(k_i+1)|k_i \quad y_{disc}(k_i+2)|k_i \cdots\cdots y_{disc}(k_i+N_P)|k_i\right]^T \qquad (31)$$
$$\Delta U_{opt} = \left[\Delta u(k_i)|k_i \quad \Delta u(k_i+1)|k_i \cdots\cdots \Delta u(k_i+N_C-1)|k_i\right]^T$$

Where $y_{disc}(k_i+m)|k_i$ is the predicted output at m^{th} sample from the present sample k_i. $\Delta u(k_i+m)|k_i$ is the optimized controlled input at m^{th} sample from the present sample k_i. N_P and N_c are the prediction horizon and control horizon. By manipulating (30) and (31) Y_{est} can be written as

$$Y_{est} = F\, x_{aug}(k) + G\Delta U \qquad (32)$$

Hence from (32) predicted output up to N_P samples from k_i instant can be written with the knowledge of the state variables at k_i sample and the optimized controlled inputs up to N_c-1 samples from k_i sample. The final objective function that determines the optimized control input vector ΔU_{opt} can be written in the quadratic form as

$$J = (R_S - Y_{est})^T (R_S - Y_{est}) + \Delta U_{opt}{}^T P \Delta U_{opt} \qquad (33)$$

Where R_S is the output reference set-point vector which contains the reference set-points for the outputs of the plant. It is to be noted that the reference set-point of a particular output is constant throughout the prediction horizon. P is the penalty factor on the input variables. After optimization at each sample an optimized ΔU_{opt} vector is generated and only that part in ΔU_{opt} that corresponds to the present sampling instant is taken as the input vector and is applied to the plant. The process is repeated for the next samples.

IV. RESULTS AND EXPLANATION

For the analysis of the capability of DMPC, it is implemented in the micro-grid shown in Fig. 2. Micro-grid differential and algebraic equations (DAE) from (2)-(28) are linearized about an operating point. Operating point used for the present study is given in APPENDIX. The linearized algebraic equations are then manipulated in such a way that the complete model of micro-grid can be expressed with the help of differential equations only. By taking a discrete time step of 20ms, the micro-grid model is expressed in discrete state space form given by (29). The input and output vectors of the plant are

$$u = \lfloor \Delta P_{ref} \quad \Delta e_{d3} \quad \Delta e_{q3} \rfloor$$
$$y = [\Delta\omega_r \quad \Delta V_3 \quad \Delta G]$$

Where $G = P_{G3} - P_{3,ref}$ in normal mode

$G = P_{G3} - \dfrac{\Delta\omega_3}{R_{D3}}$ in frequency regulation mode

G represents the role of EI-DG in the micro-grid. In steady state EI-DG generates constant active power according to its pre-set value $P_{3,ref}$. During transient state it acts in frequency regulation mode in which it adjusts its active power according to its droop characteristics given by R_{D3}.

A. Performance of MPC during load disturbances in micro-grid

A step load change of 50kW at B3 is applied at 51st sampling instant as input disturbance which is shown in Fig. 5. The output set-point reference vector (R_S) elements are taken as zeros. Control horizon and prediction horizon are taken as 2 and 4 samples respectively. The penalty factor P for every input variable is taken as 0.001. The frequency deviation of the system with DMPC is shown in Fig. 6. The peak deviation occurred is 59.9807 Hz which is well within limits of 59.93 Hz to 60.1 Hz. The frequency is restored to nominal value in 7.34 sec.

Fig. 7 shows the mechanical power output from the turbine of the SG-DG. In the steady state the mechanical input of the SG-DG is increased by 50.8 kW from 3267.5 kW to 3318.3 kW. Hence the total load change is compensated by increase in the output power of SG-DG alone in the steady state. However during transients load change is balanced by increase in mechanical output from the diesel turbine, increase in power output of the EI-DG unit and energy stored in the SG-DG inertia. Fig. 8 shows the active power output of the EI-DG unit. Before disturbance EI-DG generates constant power output of 1500 kW based on its reference active power set-point. After the disturbance occurred, during transient state it follows the droop characteristics assigned to it until the frequency is completely restored. When the frequency is restored it again switches back to its normal mode in which it follows pre- assigned active power set point.

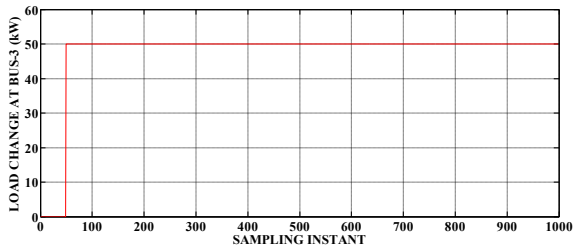

Fig. 5 Load disturbance at bus B3

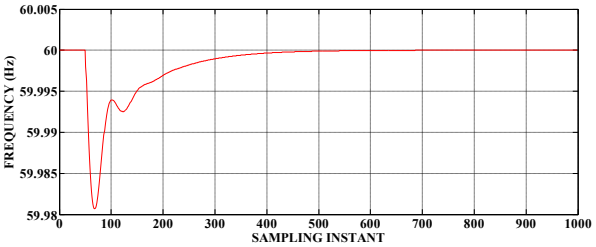

Fig. 6 Frequency of the micro-grid

Fig. 9 shows the voltage at B3. The peak voltage deviation is 0.9985 p.u. The voltage is restored to 1 p.u. in 6 samples which is 0.12 sec. The voltage is locally controlled by the EI-DG unit by generating sufficient reactive power. Hence DMPC is well suited for fast voltage recovery.

Fig. 10 shows the voltage at B1 which is controlled by the local exciter of SG-DG. Due to the slow dynamics of the exciter, voltage recovery at B1 is taking more time than the time taken by DMPC at B3.

Fig. 11 and Fig. 12 show i_{d3} and i_{q3} of EI-DG. From Fig. 11 it can be noticed that current i_{d3} is the key parameter to control active power output of the EI-DG. Before and after transient period, i_{d3} is same indicating that active power output of the EI-DG is following pre-assigned reference in steady state and droop characteristics in transient period. Reactive power injected by EI-DG can be controlled by current i_{q3}. Hence by using DMPC independent d-q current control can be achieved.

Fig. 13 and Fig. 14 compares PI control with MPC in the context of frequency and voltage control of micro-grid. Typical parameters of PI control are given in [10]. From Fig. 13 and Fig .14 it can be noticed that MPC had a better steady state performance and transient performance when compared to PI control.

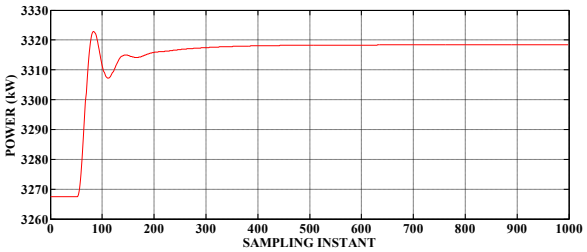

Fig. 7 Mechanical input of the SG-DG

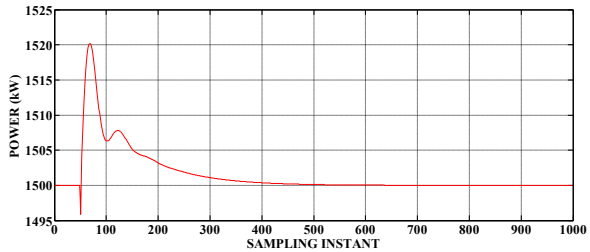

Fig. 8 active power output of EI-DG

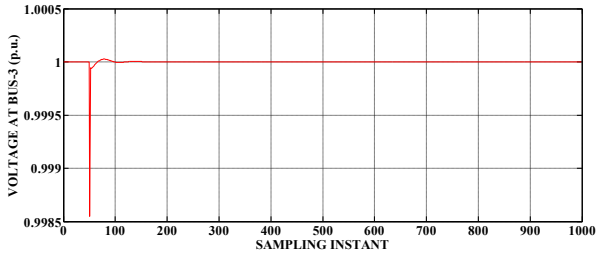

Fig. 9 Voltage at bus B3

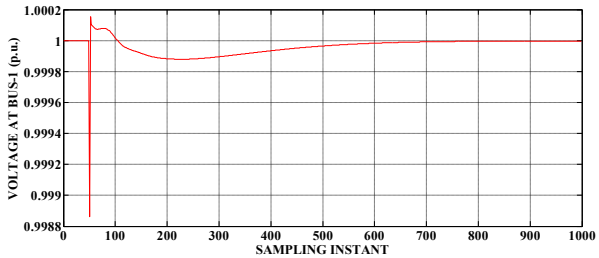

Fig. 10 Voltage at bus B1

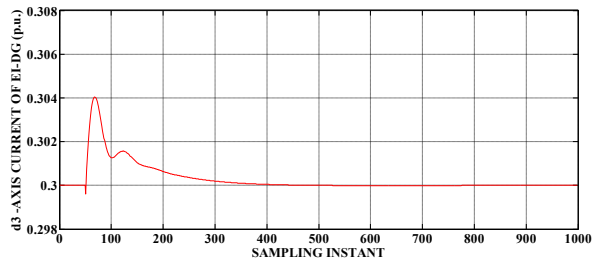

Fig. 11 d3-axis current of EI-DG

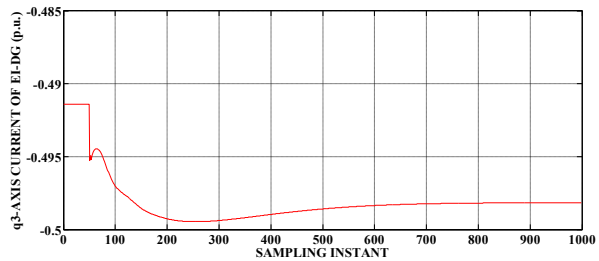

Fig. 12 q3-axis current of EI-DG

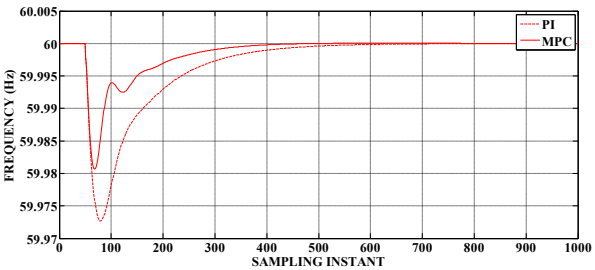

Fig. 13 Comparison of frequency control using PI and MPC

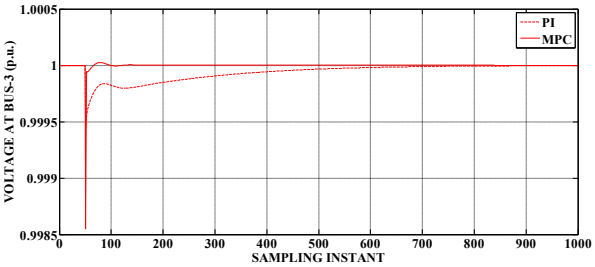

Fig. 14 Comparison of voltage control at B3 using PI and MPC

B. Impact of storage on the system

If the isolated micro-grid is equipped with a storage system, then the frequency related issues can be handled more effectively. Generally during discharging, storage and its associated inverter are forced to operate at unity power factor (UPF) so that only active power is injected into the micro-grid. While charging it acts as UPF load. Mathematical model of the MPC in the presence of the storage did not change much except that two more states, d-q axis currents of storage inverter are added to the mathematical model and the control is similar to that of the PV inverter control. However the role of the storage during a disturbance in the system is decided by the state of charge (SOC). If SOC is within limits then it is allowed to participate in frequency regulation with an emulated droop characters along with other generators in the system until its SOC reaches either maximum or minimum limits depending on the type of load disturbance. Once SOC reaches limits, then it acts as controllable UPF load.

C. Possibilities of practical implementation

The practical hardware implementation of the MPC in isolated micro-grids can be done using

- A micro-controller which uses a digital signal processor (DSP) chip. This can be implementable for small micro-grids with limited generators.
- For laboratory setups and for prototyping of real time systems, MPC can be implemented using MATLAB real time workshop and xPC target.
- For large micro-grids MPC can be implemented using a real time computer based monitoring and supervisory control system interfaced with programmable logic controller.

V. CONCLUSION

The frequency and voltage control capability of DMPC in isolated micro-grid is investigated in this study. Dynamic models of the micro-grid generators are considered for the study. Micro-grid network is represented by steady state equations. Mathematical equations of the DMPC are given in detail. Simulations are carried out using MATLAB software package. Load changes are taken as the input disturbances and the results shows that DMPC provides fast recovery of voltage and frequency. The results show that DMPC can coordinate with speed governor and excitation of the SG-DG. Simulations also show that the dynamic characteristics of DMPC are better than PI control.

APPENDIX

Operating point of the micro-grid:
$V_1 = V_3 = 1$ p.u.
$V_2 = 0.997131$ p.u.
$P_{G1} = 3.26$ MW
$Q_{G1} = 1.4652$ MVAr
$P_{G2} = 1.5$ MW
$Q_{G2} = 2.45$ MVAr
$\theta_1 = 0^0$
$\theta_2 = -0.312970^0$
$\theta_3 = -0.671047^0$

REFERENCES

[1] P. Kundur, Power System Stability and Control. New York, USA: McGraw-Hill, 1994.

[2] F. Katiraei, M. R. Iravani, and P. W. Lehn, "Small-signal dynamic model of a micro-grid including conventional and electronically interfaced distributed resources," IET Gener. Transm. Distrib., vol. 1, no. 3, pp. 369–378, May 2007.

[3] F. Katiraei, M. R. Iravani, and P. W. Lehn, "Micro-grid autonomous operation during and subsequent to islanding process," IEEE Trans. Power Del., vol. 20, no. 1, pp. 248–257, Jan. 2005.

[4] F. Katiraei and M. R. Iravani, "Power management strategies for a microgrid with multiple distributed generation units," IEEE Trans. Power Syst., vol. 21, no. 4, pp. 1821–1831, Nov. 2006.

[5] Kai Yu, Qian Ai, Shiyi Wang, Jianmo Ni, and Tianguang Lv, " Analysis and optimization of droop controller for microgrid system based on small signal dynamic model," IEEE Trans. Smart Grid, vol. 7, no. 2, pp. 695–705, Mar. 2016.

[6] C. Schauder and H. Mehta, "Vector analysis and control of advanced static VAr compensators," IEEE Proc. C Gen. Transmiss. Distrib., vol. 140, no. 4, pp. 299–306, Jul. 1993.

[7] L. Wang, Model Predictive Control System Design and Implementation Using MATLAB. Berlin, Germany: Springer-Verlag, 2009.

[8] A. M. Ersdal, I. M. Cecílio, D. Fabozzi, L. Imsland, and N. F. Thornhill, "Applying model predictive control to power system frequency control," in Proc. 2013 4th IEEE/PES Innovative Smart Grid Technologies Europe, 2013.

[9] A. M. Ersdal, L. Imsland, and K.Uhlen, "Model predictive load-frequency control," IEEE Trans. Power Syst., vol. 31, no. 1, pp.777–785, Jan. 2016.

[10] H. Xin, Y. Liu, Z. Wang, D. Gan, and T. Yang, "A New Frequency Regulation Strategy for Photovoltaic Systems Without Energy Storage," IEEE Trans. Sustain. Energy, vol. 4, no. 4, pp. 985–993, 2013.